ENVIRONMENTAL RESEARCH
COMMUNICATIONS

ACCEPTED MANUSCRIPT • OPEN ACCESS

Amplification factors for extreme sea level frequency have problematic features as a metric of coastal hazard

To cite this article before publication: Timothy M. Hall 2024 *Environ. Res. Commun.* in press https://doi.org/10.1088/2515-7620/ad431e

Amplification Factors for Extreme Sea Level Frequency have Problematic Features as a Metric of Coastal Hazard

Timothy M. Hall[1]

[1]S&P Global Sustainable 1

timothy.hall@spglobal.com

Accepted for publication in Environmental Research Communications.

Abstract. The future projected frequency of a specified baseline extreme sea level (ESL), often called the amplification factor (AF), is extensively used as a metric of evolving coastal flood hazard with sea level rise (SLR). The baseline ESL is typically analyzed using extreme value analysis, and the SLR is added to the resulting ESL distribution. In the presence of uncertainty in SLR, it is natural to analyze projected AFs probabilistically. I derive probability density functions (PDFs) of AF, given uncertainty distributions of SLR. If the ESL distribution is modeled as Gumbel and the SLR distribution as normal, then the AF distribution is log normal. However, in active tropical cyclone regions, ESL often has a longer tail than Gumbel, and a Frechet (Type-II) Generalized Extreme Value (GEV) is more appropriate. In this case, I shown that the AF distribution has a divergent mean. In addition, I show that for Frechet ESL, the AF cannot even be defined for SLR above a threshold $(\beta/\xi)f_0^{-\xi}$, where f_0 is the specified baseline frequency (e.g., f_0 = 0.01 yr^{-1} for the 100-year exceedance), β is the GEV scale parameter and ξ the shape parameter. Above this SLR threshold, ESL at all frequencies exceeds the baseline reference frequency, preventing the calculation of AF. The resulting probabilistic distribution of AF has no sensitivity to SLR above the threshold. These features detrimentally impact the utility of AF as a hazard metric. Frechet distributions are appropriate and commonly used for ESL in tropical cyclone regions, but AFs applied to such distributions need to be interpreted with caution.

1 Introduction

Extreme sea level (ESL), exceptionally high coastal water levels caused by tides and storm surge (Gregory et al, 2019), is a major driver of coastal flooding. Sea-level rise (SLR) exacerbates flooding due to coastal storm tide by increasing the background water level on top of which the storm tide propagates. Research in projecting future storm tide levels with SLR is extremely active (e.g., Oppenheimer et al, 2019; Kireczi et al., 2020; Sweet et al., 2022), and calculating coastal flood loss in response to storm tide and SLR is a crucial component of climate risk analysis.

A widely used metric of the evolving hazard is the future projected frequency in the exceedance of a specified historical ESL. For example, the specified ESL might be the level that was exceeded historically with an average annual frequency of 0.01 yr^{-1} (the "hundred-year level"), while at a future SLR level that same ESL might be exceeded with a frequency of 0.03 yr^{-1}. The fractional change, in this case 3, is often termed the amplification factor (AF). The conclusions made here apply equally to the projected frequency and the AF, as their difference, multiplication by a constant reference frequency, is immaterial. Frequency and AF terminology are both used here.

Examples of the use of AF are numerous. Lin et al (2016) projected increased annual frequencies of exceeding Hurricane Sandy's storm-tide level on New York City. Vitousek et al (2017) estimated AFs globally to the baseline 50-year exceedances, including waves, and showed that regions with relatively smaller historical ESL variations have the greatest AFs. Rasmussen et al. (2018) use AFs to examine SLR impacts under several temperature stabilization targets. Ghanbari et al (2019) developed a statistical model encompassing both nuisance and extreme coastal flood on the US, using AFs as the metric for their projected increase in hazard. The IPCC 2019 report on oceans and the cryosphere summarized changes in coastal ESL in part with AFs (Oppenheimer et al, 2019). Frederikse et al (2020) concluded that tropical coastal sites are especially susceptible to increased frequency of the historical 100-year ESL, with many such sites even having mean sea level above the 100-year reference level by 2100. Taherkhani et al (2020) concluded that many US coastal regions experience approximately exponential increase in AF of the baseline 1-in-50-year frequency. Rashid et al (2021) used AFs to diagnose the large impacts of interannual and decadal variability on ESL, while Tebaldi et al (2021) identified global warming levels beyond which coastal regions will experience historical 0.01 yr^{-1} frequencies daily. Finally, Hermans et al (2023) estimated future years at which AFs exceed regional flood protection standards.

SLR projections have many sources of uncertainty (Kopp et al, 2023), and this uncertainty impacts AF. All the studies listed above acknowledge the large uncertainty in SLR projections and, at least qualitatively, the impact that uncertainty has on AFs. A smaller number of studies have propagated probabilistic SLR descriptions to probabilistic AF. Buchanan et al. (2017) use uncertainty distributions of SLR to infer distributions of AF. Howard and Palmer (2020) and Goodwin et al (2017) analyze AF distributions and their means. Components of the work of Goodwin et al (2017) and Howard and Palmer (2020) are based on the theoretical work of Hunter (2012). Strictly speaking, the results from Hunter (2012) are limited to Gumbel ESLs, but Goodwin et al (2017) and Howard and Palmer (2020) generalize certain aspects beyond Gumbel.

Here, I address the impact of probabilistic descriptions of SLR on probabilistic descriptions of projected frequency (and therefore, AF). I show that AF has two features that compromise its use as a coastal hazard metric. These features arise in regions with episodic intense ESL, such as tropical cyclone regions, where the ESL distribution is commonly and appropriately summarized with heavy-tailed Frechet (Type II) GEV distributions (e..g., Tebaldi et al., 2012; Zervas, 2013; Marcos and Woodworth, 2017). Firstly, in such regions, the AF has a distribution whose tail is heavy enough that the mean AF mean is infinite. Any practitioner of coastal-risk analysis who uses AF as a hazard metric under SLR and seeks to incorporate uncertainty probabilistically will be stymied in attempts to estimate mean AF. Secondly, for Frechet ESL, AF cannot be defined for SLR above certain thresholds determined by the GEV parameters, and these threshold SLRs are well within reach by late 21st century. For SLRs above threshold, ESL at all frequencies is higher than the baseline ESL of the specified reference return period. This feature severely hampers AF as a hazard metric for ESL under SLR, at least in active tropical cyclone regions.

The paper is organized as follows: First, the relationship between ESL and annual occurrence frequency in terms of GEV parameters is motivated. Then, I derive probability density functions (PDFs) of AF, assuming uncertainty distributions of SLR. In the case of Frechet (Type-II) GEV ESL, the mean of the AF PDF is divergent. In addition, it is shown that AF cannot be defined for SLR above a threshold value determined by the GEV parameters. I then conclude with discussion on the relevance of the results to diagnosing ESL hazard.

2 Occurrence Frequency and GEV Parameters

This section motivates the relationships between an ESL value, X, and the annual frequency of ESL exceeding X. These relationships can be found, for example, in Hunter (2012) in the Gumbel case and Palutikof et al (1999) in the GEV case. However, it is useful for subsequent development to derive the results in the current context.

The GEV distribution is derived from a Poisson process for an event having a maximum value *X'* exceeding *X* in interval τ. Thus, the probability of waiting longer than one year between events exceeding *X* is

$$P(T > 1) = e^{-f\tau} \quad (1)$$

where *f* is the average number of events exceeding *X* in the interval τ. This is the equal to the probability that no event exceeds *X* in τ. We are interested in annual rates, and henceforth we use $\tau = 1$ year henceforth.

Consider the GEV distribution for the maximum annual exceedance level X. The probability of maximum X' less than *X* is the GEV CDF at *X*:

$$P(x' < x) = \exp\left(-t(X)\right) \quad (2)$$

where $t(X) = (1 + \xi\alpha)^{-1/\xi}$, $\alpha = (X - \mu)/\beta$, μ is the location parameter, β is the scale parameter, and ξ is the shape parameter. The probability of annual maxima less than *X* equals the probability that no event exceeds *X*. Thus, (1) and (2) can be equated. Solving for *X* yields

$$X = \mu + \beta\left(\frac{f^{-\xi}-1}{\xi}\right) \quad (3)$$

In the limit, $\lim_{\xi\to 0}\left(\frac{f^{-\xi}-1}{\xi}\right) = -\ln(f)$, and the Gumbel version of (3) is $X = -\beta\ln(f) + \mu$.

The timescale $1/f$ is not the return period. The return period is the reciprocal of the annual probability of at least one exceedance, and therefore cannot be less than one year. By contrast, $1/f$ is the average time between successive exceedances, sometimes called the average recurrence interval (ARI), and $1/f$ can assume any positive value. It may seem counterintuitive to consider values $f > 1$ yr^{-1} (ARI < 1 yr) in the context of GEV for annual exceedances. The GEV is constructed from time series of annual maxima, and the GEV cumulative distribution function (CDF) is the probability *p(X)* that the maximum annual ESL is less than *X*. However, there is no contradiction. The GEV CDF at *X* is the probability that the maximum annual value *X'* is less than *X*, even when the underlying average frequency, *f*, of exceeding *X*, is high, including $f > 1$ yr^{-1}. That is, there is non-zero probability that the maximum *X'* in a year is less than *X*, even when the annual frequency of exceeding *X* is greater than 1 yr^{-1}.

2. Relating SLR Distributions to Projected Frequency Distributions

The PDF of the projected annual frequency of storm-tide induced coastal ESL is now derived, assuming a GEV PDF for the historical baseline period and normally distributed uncertainty on SLR. SLR has many sources of uncertainty, both quantifiable and unquantifiable (Kopp et al, 2023), and a number of studies argue compellingly for non-normal skewed SLR distributions driven in large part by uncertain ice sheet decline (de Winter et al, 2017; Bamber et al., 2019; Robel et al., 2019). The purpose here is to make certain general observations about the impact on AF of the combination of SLR distributions and GEV ESL. The conclusions that, for a Frechet GEV ESL, the mean AF diverges is true for a range of SLR distributions, as discussed subsequently in Section 5. Moreover, the conclusion that the AF cannot be defined for SLR above a certain threshold is independent of the SLR distribution. However, to illustrate with an analytic frequency PDF, a normal distribution of SLR is assumed.

The linearity between *X* and $(f^{-\xi} - 1)/\xi$ in equation (3) allows a straightforward derivation of a frequency PDF. In Fig 1a, the baseline linear relationship between *X* and $(f^{-\xi} - 1)/\xi$ is shown. Also shown is the reference ESL, X_0, corresponding to the reference frequency, f_0 (e.g., $f_0 = 0.01$ yr^{-1} for the reference 100-year ESL exceedance). In Fig 1b, the baseline ESL curve is shifted upward by a mean SLR, μ_{SLR}, and the new value, μ_f, of $(f^{-\xi} - 1)/\xi$ that corresponds to the same exceedance X_0 is shifted leftward. The linear geometry can be used to infer μ_f . The slope of the curve, β from equation (3), can be seen from Fig 1b to be μ_{SLR}/Δ, where $\Delta = \left(\left(f_0^{-\xi} - 1\right)/\xi - \mu_f\right)$. Equating μ_{SLR}/Δ to β and solving for μ_f yields

$$\mu_f = \left(\frac{f_0^{-\xi} - 1}{\xi}\right) - \frac{\mu_{SLR}}{\beta} \tag{4}$$

In Fig 1c, the ESL curve is shifted upward in addition by one standard deviation, σ_{SLR}, in SLR. The increase induces a further leftward shift in the $(f^{-\xi} - 1)/\xi$ that corresponds to the same X_0. Similar to the mean μ_f, the standard deviation, σ_f, in $(f^{-\xi} - 1)/\xi$ corresponding to σ_{SLR} can be inferred from the linear geometry. From Fig 1c, the slope β is σ_{SLR}/σ_f, and therefore

$$\sigma_f = \frac{\sigma_{SLR}}{\beta} \tag{5}$$

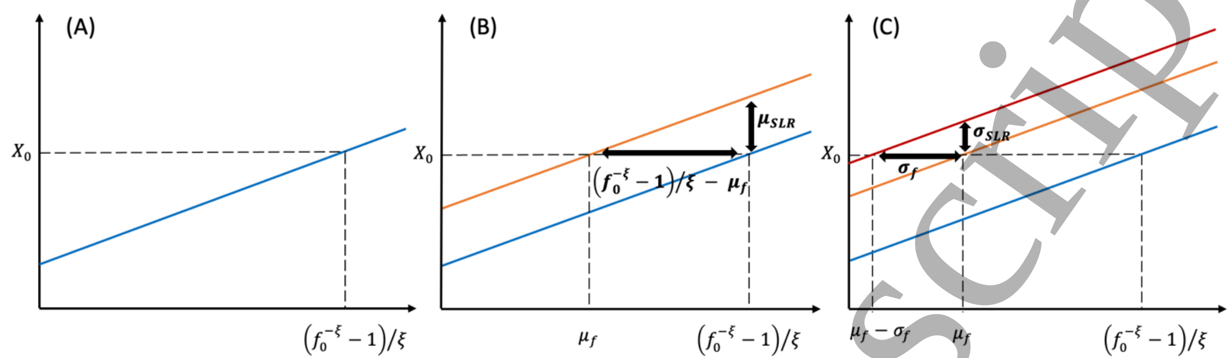

Fig 1: Graphical illustration relating ESL with SLR to frequency. ESL is plotted as its linear function of $\left(f^{-\xi}-1\right)/\xi$ from equation (3), with slope β. (A) The baseline relationship (blue), with the ESL, X_0, corresponding to the reference frequency f_0 indicated by dashed lines. (B) A mean value of SLR, μ_{SLR}, is added to the baseline (orange), shifting the curve upward. The new value, μ_f, of $\left(f^{-\xi}-1\right)/\xi$ corresponding to the same baseline X_0 is indicated by the second dashed line. The shift in $\left(f^{-\xi}-1\right)/\xi$ is equal to $\Delta=\left(f_0^{-\xi}-1\right)/\xi\ -\mu_f$. (C) A standard deviation in SLR, σ_{SLR}, is added (red), shifting the curve further upward. The additional shift leftward, σ_f, in $\left(f^{-\xi}-1\right)/\xi$ that corresponds to the same baseline X_0, is indicated by the third dashed line.

Because of the linearity of the ESL curve and the assumption of normally distributed SLR, the distribution of $\left(f^{-\xi}-1\right)/\xi$ values that corresponds to X_0 is also normal. Thus, the PDF for the variable $g(f)\equiv\left(f^{-\xi}-1\right)/\xi$ is normal with mean μ_f and standard deviation σ_f. To convert to a PDF in f, note that

$$\int_0^{+\infty}p(g)dg\ =-\int_{+\infty}^{0}p(g(f))\,\frac{dg}{df}df\ =\ \int_0^{+\infty}p(g(f))\,f^{-\xi-1}df\ =\ 1 \qquad (6)$$

Therefore,

$$p(f)=p(g(f))f^{-\xi-1} \qquad (7)$$

Or, with the normal SLR distribution,

$$p(f)\ =\frac{f^{-\xi-1}}{\sigma_f\sqrt{2\pi}}\exp\left(-\frac{1}{2}\left(\frac{\left(\frac{f^{-\xi}-1}{\xi}\right)-\mu_f}{\sigma_f}\right)^2\right) \qquad (8)$$

In the limit $\xi \rightarrow 0$, the GEV is Gumbel, and (8) is log normal. Examples of PDF (8) are shown in Fig 2. Note that this PDF can readily be re-expressed in terms of AF by simply replacing f with $AF \times f_0$.

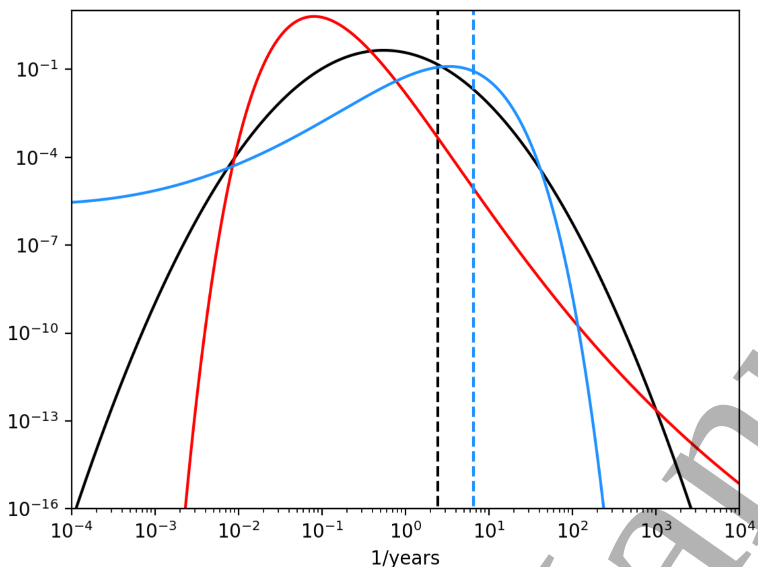

Fig 2: Examples of frequency PDF of equation (8). Black is the Gumbel-derived frequency PDF (log-normal, ξ=0), red is derived from GEV with ξ=0.2 (Frechet), and blue is derived from GEV with ξ=-0.2 (Weibull). The corresponding black and blue vertical dashed lines indicate the mean frequencies, 2.4 yr^{-1} (Gumbel) and 6.5^{-1} years (Weibull). For Frechet, the mean of the frequency PDF is infinite. The reference frequency in this example is f_0 = 0.01 yr^{-1}.

3. Divergent Mean for Frechet GEV

For the Frechet GEV realm (0<ξ<1), the frequency PDF (8) has an infinite mean. This can be seen by noting that, in the limit of large f, the argument in the exponent approaches a finite value. Meanwhile, the pre-factor varies as $f^{-(\xi+1)}$. Thus, in computing the mean, the integrand of the first moment, $f\,p(f)$, limits to $f^{-\xi}$, which results in divergence for ξ<1. The long tail is illustrated by comparing Fig 3, the Gumbel ESL case, and Fig 4, the Frechet case. Both figures show a series of SLR increments (the parallel curves) and the corresponding series of frequencies that result in the same baseline ESL (the vertical dashed lines). If the SLR distribution is assumed normal, then the distribution of log(f) for Gumbel ESL (Fig 3) is also normal, as the ln(f) values corresponding to X_0 (vertical dashed lines) are equally spaced. For Frechet (Fig 4), however, the ln(f) corresponding to the same X_0 (vertical dashed lines) bunch together at small ln(f) and expands at large ln(f), resulting in a longer tail than the Gumbel case. The projected frequencies (and hence AF) increase rapidly enough that the mean of the PDF diverges. (As shown below in Section 5, the divergence occurs for a wide range of SLR distributions, not just normal.)

Several studies have hinted at the divergence of mean AF. Vitsousek et al (2017) and Buchanan et al (2017) noted the high sensitivity of AF to GEV parameters, especially the shape parameter. They also note the fact that mean of the AF distribution is greater than the AF in response to the mean SLR. Buchanan et al (2017) calculated a mean AF in response to the SLR uncertainty distributions of Kopp et al (2014), showing strong sensitivity of the mean to the SLR uncertainty. Rasmussen et al (2018) estimated extremely high AFs in Kushimoto, Japan, where the ESL distribution is heavy tailed. For example, AF=1462 by 2100 for the reference 10-year ESL and AF=41479 for the reference 500-year ESL (2.0°C stabilized global mean surface temperature increase). Rasmussen et al (2018) further note that their AF estimates are sensitive to truncations in the uncertainty sampling scheme and may not converge within their truncated range.

I am not aware, however, of the divergence of the mean AF for the Frechet GEV being made explicit previously. The divergence is a consequence of analyzing the distributional frequency response to an uncertainty distribution of SLR, combined with a positive shape parameter (Frechet) in the ESL GEV distribution. Frechet distributions have to be interpreted with caution. As noted by Vitousek et all (2017), positive shape parameter for ESL does not respect physical upper bounds on surge and tide. Statistical fits of storm tide with positive shape parameter are driven by the presence of outlier ESL in finite time series, for example, from rare and extreme tropical cyclones. With physical upper bounds enforced, the tail of the ESL distribution would be truncated, and the mean AF would be finite. However, the mean would still depend on the poorly known storm-tide upper bounds.

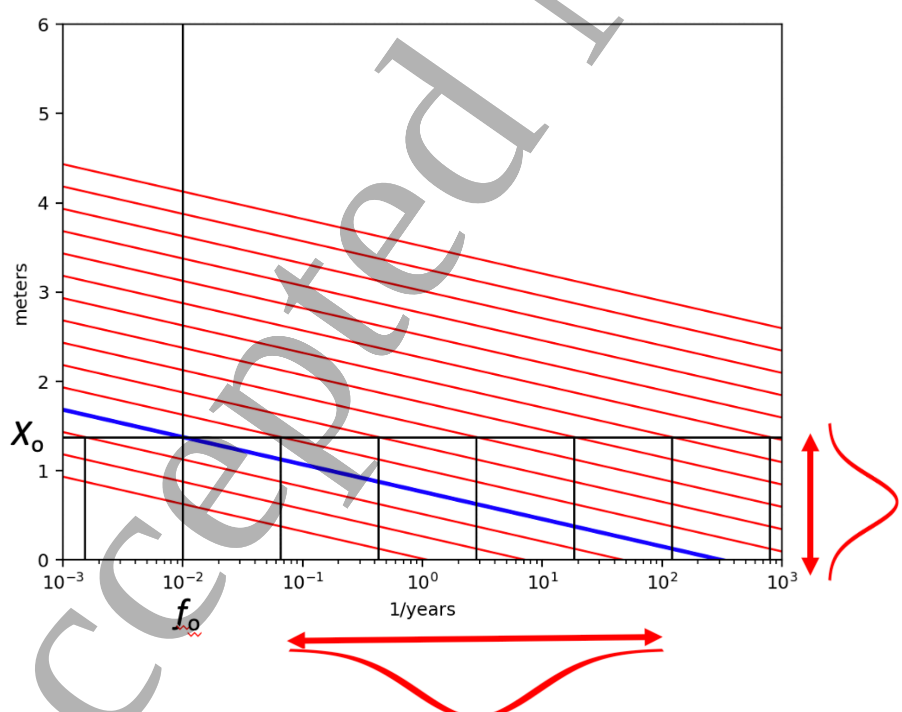

Fig 3: ESL versus log frequency for a Gumbel fit by Zervas (2013) for Boston, MA (μ_0=0.764m, β=0.133m). The baseline ESL curve is shown blue, and projected SLR in 0.25m increments from the baseline (including negative SLR) are shown red. The SLR values are imagined to be distributed normally, as indicated schematically by the distribution on the right. The tall vertical black line indicates the reference frequency, f_0 = 0.01 yr^{-1}. The horizontal black line indicates the baseline reference ESL, i.e., the ESL X_0 that is exceeded annually with frequency f_0, here about 1.34m. The short vertical lines indicate the projected frequencies that correspond to X_0 for the various SLR increments. Due to the log-linearity of the relationship, the frequency distribution is also normal in ln(f), as indicated schematically by the distribution below; i.e., it is log-normal in f.

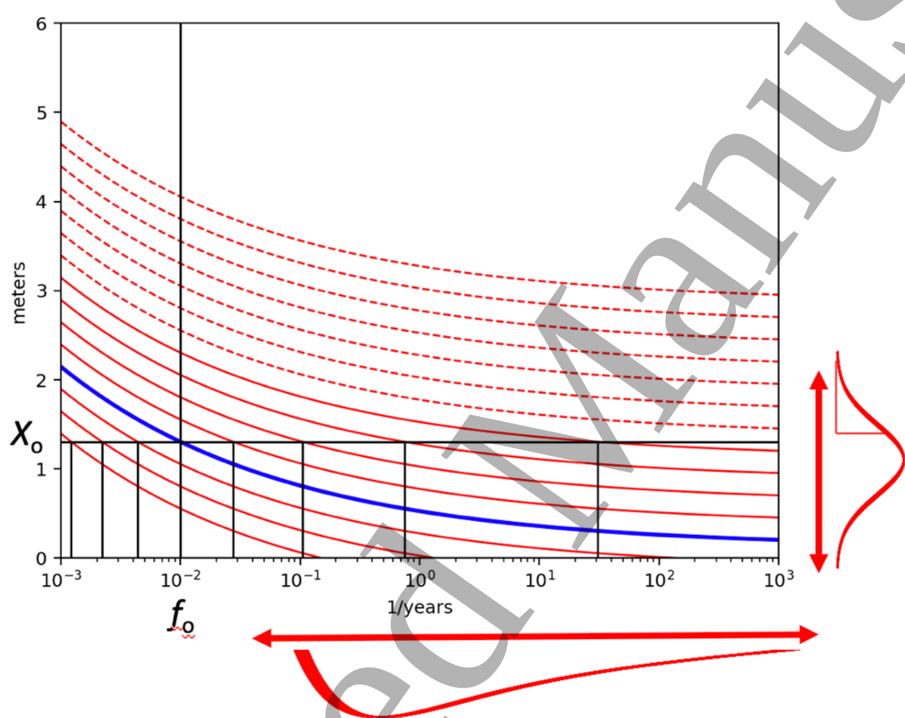

Fig 4: As in Fig 3, but here for an example of Frechet GEV ESL, taken from Zervas (2013) for Charleston, SC (μ_0=0.526m, β=0.094m, and ξ=0.234), with X_0 = 1.30m. Compared to the Gumbel example of Fig 3, here the relationship is not log-linear, but is instead increasingly shallower with f. As SLR increases, the frequencies that correspond to the baseline ESL exceedance X_0 are increasingly more widely spaced, and the log-frequency distribution is skewed to heavy tails, as illustrated in the distribution at bottom. In addition, there is a critical SLR increment above which the ESL curve never reaches as low as X_0. At SLR above this threshold (about 1.18m in this example) future ESL is higher than the reference ESL at all frequencies. ESL curves above this threshold are indicated with dashed lines. A truncation is shown in the normal SLR distribution at left, indicating the SLR values to which the frequency is not sensitive.

4. Limit on SLR Sensitivity for Frechet GEV

The Frechet GEV has a minimum allowed ESL exceedance value. In the limit of high frequency, equation (3) has the minimum X of

$$X_{min} = \mu - \frac{\beta}{\xi} \tag{9}$$

In the frequency PDF (8), as f ranges from zero to infinity, the associated X ranges from infinity to X_{min}. As seen in Fig 4, when X_{min} exceeds the historical baseline reference ESL, X_0, no projected future frequency exists that generates the ESL X_0. This implies an upper threshold value of SLR, above which a projected frequency corresponding to X_0 cannot be found, an AF cannot be defined, and further SLR cannot influence the frequency (or AF) PDF. To obtain this threshold, consider the reference ESL from equation (3)

$$X_0 = \mu + \beta \left(\frac{f_0{}^{-\xi} - 1}{\xi}\right) \tag{10}$$

where f_0 is the reference frequency, e.g., $f_0 = 0.01$ yr^{-1} for the 100-yr exceedance. With SLR, the location parameter shifts from its baseline value, μ, to $\mu + \mu_{SLR}$, and X_{min} becomes

$$X_{min} = \mu + \mu_{SLR} - \frac{\beta}{\xi} \tag{11}$$

X_{min} increases with SLR. Once X_{min} exceeds X_0, there is no projected frequency that can produce X_0. Above that threshold value of X_{min}, all frequencies result in X above X_0. The upper portion of the SLR distribution, where $X_{min} > X_0$, does not impact on the frequency (or AF) distribution. The threshold X_{min} occurs when

$$X_{min} = \mu + \mu_{SLR} - \frac{\beta}{\xi} = X_0, \tag{12}$$

Solving for the threshold SLR,

$$\mu_{SLR} = X_0 - \mu + \frac{\beta}{\xi} \tag{13}$$

Finally, substituting from (10) for X_0 yields:

$$\mu_{SLR} = \frac{\beta}{\xi} f_0^{-\xi} \tag{14}$$

This threshold SLR, above which no AF can be defined, and no contributions are made to the frequency distribution, depends only on the baseline GEV scale and shape parameters. Fig 4 illustrates the threshold magnitude with GEV parameter values from Table A of Zervas (2013) for Charleston, South Carolina: $\beta = 0.094$m and $\xi = 0.234$. For the

100-yr reference ($f_0 = 0.01\text{yr}^{-1}$), this gives $\mu_{SLR} = 1.18$m. Further SLR above 1.18m does not contribute to the AF PDF. Thus, for typical observationally estimated Frechet GEV parameters, a threshold SLR, above which AF cannot be defined, is well within range of projected values for late century.

Note that in the Gumbel limit of (3) ($\xi \rightarrow 0$), the threshold SLR is infinite. All SLR contribute to the Gumbel frequency distribution. The threshold SLR issue does not arise, as $X = \mu - \beta \ln(f)$ has no lower bound on X.

5. Other SLR Distributions

The existence of an upper SLR threshold of frequency-distribution sensitivity does not depend on the nature of the SLR distribution. The steps to obtain the threshold (14) depend only on the existence of a minimum ESL, X_{min}. The divergence of the mean projected frequency is also largely independent of the SLR distribution. To see this, note that in equation (7), as f increases, X limits to X_{min} and $g(f)$ limits to $-1/\xi$. Therefore, if the SLR PDF is nonzero at X_{min}, then $p(g(f))$ is nonzero, and the PDF (7) limits to $f^{\xi-1}$. As before, the integrand of the first moment then limits to $f^{-\xi}$, which diverges for $0<\xi<1$. In other words, if the ESL is Frechet distributed and there is non-zero probability of SLR above $(\beta/\xi)f_0^{-\xi}$, then the mean projected frequency is infinite.

6. Discussion and Conclusions

In many coastal regions, such as those with tropical cyclone activity, extreme sea levels (ESL) are best described by a Frechet GEV distribution, which has a longer tail than the Gumbel distribution. Sea level rise (SLR) increases the frequency of ESLs above a given threshold, with the fractional frequency change termed the amplification factor (AF). SLR has uncertainty, and this translates to an uncertainty distribution of AF.

I have derived certain properties of AFs with Frechet ESL distributions that compromise AF as a coastal hazard metric in this context:

1. AF cannot be defined when SLR is above the value $(\beta/\xi)f_0^{-\xi}$, where f_0 is the baseline frequency specifying the reference ESL (e.g., $f_0 = 0.01$ yr^{-1} for the 100-year exceedance), β is the GEV scale parameter and ξ the shape parameter. For higher SLR, all frequencies result in ESL above the reference ESL.
2. If an SLR uncertainty probability density function (PDF) is used to derive a corresponding uncertainty PDF for AF, then the AF PDF is not sensitive to SLR values above the threshold $(\beta/\xi)f_0^{-\xi}$.
3. If the SLR uncertainty PDF has non-zero probability above $(\beta/\xi)f_0^{-\xi}$, then the mean AF (first moment of the AF PDF) is infinite.

Typical values of the SLR threshold $(\beta/\xi)f_0^{-\xi}$ are well within range for the end of century, e.g., an estimated threshold of 1.18 m in Charleston, SC. Therefore, these features may limit the utility of projected frequency (and AF) as a diagnostic of coastal flood hazard metric under SLR, at least in regions of large episodic ESL, such as tropical cyclone regions, where Frechet GEV is appropriate. A divergent mean AF is merely inconvenient. An infinite mean of a distribution is not a particularly useful summary, but other summaries, such as the mode and median, are still available. The threshold SLR above which AF cannot be defined is more problematic. Any coastal-risk practitioner using AFs in such a situation would find that AF values get arbitrarily large before the SLR of interest is reached, and then cannot be determined above the SLR threshold. One would like a diagnostic of coastal hazard under SLR to be sensitive to the full plausible range of SLR. If it is not, the diagnostic has limited utility.

AFs have other clear limitations as coastal hazard metrics. As highlighted by Rasmussen el al (2022), AFs are derived exclusively from the physical hazard, extreme sea level. They don't take into account the exposure and vulnerability necessary to estimate risk. Even as a hazard metric, AFs alone don't indicate the absolute ESL value, only its frequency change. For example, a 100-year AF of 10, indicating a 10-fold increase in frequency of the reference 100-year ESL exceedance, may have no bearing on hazard if that reference ESL amounts to negligible flood depth. This is partly because AFs only measure change in ESLs at the coast, without taking into account flow pathways and elevation (e.g., Rasmussen et al, 2022). The theoretical analysis here has shown that, when applied to Frechet (long-tailed) ESL distributions, AFs have additional limitations based purely on their mathematical properties. Caution is therefore advised in the use of AFs as a hazard diagnostic in active tropical cyclone regions, where Frechet GEV ESLs are appropriate.

Data Availability

The work is theoretical in nature, and no data were used.

Author Contribution

TH performed the analysis, produced the figures, and prepared the manuscript.

Competing Interests

The author declares that he has no conflicts of interest.

Acknowledgements

The author acknowledges helpful discussions with Terence Thompson, Kimberley Drouin, Danielle Montagne, and Simon Parkinson of S&P Global, as well as James Kossin of the University of Wisconsin, Hun Baek of Yale University, and William Sweet of NOAA. Comments from two anonymous reviewers significantly improved the manuscript. The work was supported by Sustainable 1, a division of S&P Global.

References

Bamber J. L., et al.: Ice sheet contributions to future sea-level rise from structed expert judgment, Proc. Natl. Acad. Sci., 116, 11195-11200, 2019.

Buchanan, M. K., et al.: Amplification of flood frequencies with local sea level rise and emerging flood regimes, Environ. Res. Lett., 12, 064009, 2017.

De Winter, R. C., et al.: Impact of asymmetric uncertainties in ice sheet dynamics on regional sea level projections, Nat. Hazards Earth Syst. Sci., 17, 2125-2141, 2017.

Frederikse, T., et al.: Antarctic ice sheet and emission scenario controls on 21st-century extreme sea-level changes, Nature Comm., 11:390, 2020.

Ghanbari, M, et al.: A coherent statistical model for coastal flood frequency analysis under nonstationary sea level conditions, Earth's Future, 7, 162-177, 2019.

Goodwin, P., et al.: A new approach to projecting 21st century sea-level changes and extremes, Earth's Future, 5, 240-253, 2017.

Gregory, J.. M., et al.: Concepts and terminology for sea level: mean, variability and change, both local and global, Surv Geophys, 40, 151-1289, 2019.

Hermans, T. H. J., et al.: The timing of decreasing coastal flood protection due to sea-level rise, Nature Climate Change, https://doi.org/10.1038/s41558-023-01616-5, 2023.

Howard, T., and M. D. Palmer: Sea-level rise allowances for the UK, Environ. Res. Comm., 2, 035003, 2020.

Hunter, J.: A simple technique for estimating an allowance for uncertain sea-level rise, Climatic Change, 113, 239-252, doi:10.1007/s10584-011-0322-1, 2012.

Kirezci, E., et al.: Projections of global-scale extreme sea levels and resulting episodic coastal flooding over the 21st century, Sci. Rep., 10, 11629, 2020.

Kopp, R. E., et al.: Probabilistic 21st and 22nd century sea-level projections at a global network of tide-gauge sites, Earth's Future, doi:10.1002/2014EF000239, 2014.

Kopp, R. E., et al.: Communicating future sea-level rise uncertainty and ambiguity to assessment users, Nature Climate Change, 13, 648-660, 2023.

Lin, N. et al.: Hurricane Sandy's flood frequency increasing from 1800 to 2100, Proc. Natl. Acad. Sci, 113, 12071-12075, doi:10.1073/pnas.1604386113, 2016.

Marcos, M., and P. L. Woorworth: Spatiotemporal changes in extreme sea levels along the coasts of the North Atlantic and the Gluf of Mexico, J. Geophys. Res. Oceans, 122, 7031-7048, 2017.

Oppenheimer, M. et al.: Sea Level Rise and Implications for Low-Lying Islands, Coasts, and Communities. In: *IPCC Special Report on the Ocean and Cryosphere in a Changing Climate*, Portner et al, (eds), Cambridge University Press, Cambridge, UK, and New York, NY, USA, pp.321-445, 2019.

Palutikof, J. P., et al.: A review of methods to calculate extreme wind speed, Meteorol. Appl., 6, 119-132, 1999.

Rashid, M. M., et al.: Extreme sea level variability dominates coastal flood risk changes at decadal time scales, Environ. Res. Lett., 16, 024026, 2021.

Rasumssen, D. J., et al.: Extreme sea level implications of 1.5°C, 2.0°C, and 2.5°C temperature stabilization targets in the 21st and 22nd centuries, Environ. Res. Lett., 13, 034040, 2018.

Rasmussen, D. J., et al: Popular extreme sea level metrics can better communicate impacts, Climatic Change, 170, 30, 2022.

Robel, A. A., et al.: Marine ice sheet instability amplifies and skews uncertainty in projection of future sea-level rise, Proc. Natl. Acad. Sci., 116, 14887-14892, 2019.

Sweet, W. V., et al.: Global and Regional Sea Level Rise Scenarios for the United States: Updated Mean Projections and Extreme Water Level Probabilities Along US Coastlines. NOAA Tech. Rep. NOS 01. National Oceanic and Atmospheric Administration, National Ocean Service, Silver Spring MD, 111 pp.

Taherkhani, M., et al.: Sea-level rise exponentially increases coastal flood frequency, Nature Sci. Rep., 10:6466, doi:10.1038/s41598-020-62188-4, 2020.

Tebaldi, C., et al.: Modelling sea level rise impacts on storm surge along the US coasts, Env. Res. Lett, 7, 014032, 2012.

Tebaldi, C., et al.: Extreme sea levels at different global warming levels, Nature Climate Change, https://doi.org/10.1038/s41558-021-01127-1, 2021.

Vitousek, S., et al.: Doubling of coastal flooding frequency within decades due to sea-level rise, Nature Sci. Rep., 7, 1399, doi:10.1038/s41598-017-01362-7, 2017.

Zervas, C.: Extreme Water Levels of the United States 1893-2010, NOAA Tech. Rep. NOS CO-OPS 067, National Oceanic and Atmospheric Administration, National Ocean Service, Silver Spring MD, 121 pp.